

# 1 Measurement based threat aware drone base station deployment

2 Alper AKARSU \*, Tolga GİRİCİ

Department of Electrical and Electronics Engineering, Faculty of Engineering, TOBB ETU, Ankara, Turkey

---

Received: .201 • Accepted/Published Online: .201 • Final Version: ..201

---

3 **Abstract:** Unmanned aerial vehicles are gaining importance with many civilian and military applications. Especially the  
4 surveillance, search/rescue and military operations may have to be carried out in extremely constrained environments.  
5 In such scenarios, drone base stations (DBSs) have to provide communication services to the people at the ground.  
6 The ground users may have no access to the global positioning system (GPS), therefore their locations have to be  
7 estimated using alternative techniques. Besides there may be threats in the environments, such as shooters. In this  
8 work, we address the problem of optimal DBS deployment under aforementioned constraints. We propose a novel DBS  
9 deployment algorithm that uses estimated positions of ground users and threats. The proposed algorithm is based  
10 on receiver signal strength (RSS) based maximum likelihood (ML) estimate of user locations and K-means clustering  
11 supported heuristic that takes into account the positions of threats. Numerical results show that proposed algorithm  
12 performs close to the computation intensive near-optimal algorithm and strikes a good trade-off between the number of  
13 unserved users and the probability of DBSs not being hit.

14 **Key words:** Drone base stations, tactical networks, metaheuristic, urban warfare

## 15 1. Introduction

16 The world's population is becoming more and more urbanized each year. As stated in the United Nation's  
17 report, 30% of world's population was urban in 1930 and it is projected that 66% of world's population will  
18 be urbanized by 2050 [1]. The urbanization process brings some potential threats to the peace of society. The  
19 demand for limited resources such as water, energy and food creates pressure to the system. This may result in  
20 the increase of unrest and violence in society and require military interventions in order to provide stability in  
21 densely populated regions. However, current military doctrines do not sufficiently recognize the challenges of  
22 conducting operations in urban environments [2]. Considering the necessity of urban warfare in future conflicts,  
23 NATO examines the impact of urban operations on the military and seeks to identify possible gaps in training,  
24 requirements and capabilities.

25 There are key factors, which make the operation in urban battlefield challenging. Intelligence collection  
26 is difficult and most of the time human intelligence [3] is needed regarding the activities of adversaries. The  
27 presence of civilians in the operation area necessitates precision fire to prevent loss of civilian life. As the  
28 urban operations are ground-intensive, maneuver warfare tactics are very difficult to apply. Last but not least  
29 challenge is the provisioning of a reliable communication network for allied forces [3, 4].

30 Establishing and maintaining a wireless battlefield communication network is a challenging task. Ter-  
31 restrial communication suffers from non-line-of-sight (NLoS) and deployment of relays or base stations poses

---

\*Correspondence: aakarsu@etu.edu.tr

1 difficulties, along with the security risks. In addition to this, mobility of friendly forces on the battlefield con-  
 2 tinuously affects the network coverage performance, hence the repositioning of communication equipments is  
 3 required. However, as the ground intensive urban combat restricts the area for deployment, the equipments may  
 4 not be placed at the appropriate locations [3]. Furthermore, the selection of the suitable position requires the  
 5 location information of the soldiers. However, the presence of widely available and inexpensive global position-  
 6 ing system (GPS) jammers may prevent the sharing of position information. In order to mitigate the effects of  
 7 GPS jamming, researchers focus on the development of anti-jamming GPS system equipped with antenna arrays  
 8 and advanced signal processing algorithms such as beamforming and spatial filtering [5]. However, design of an  
 9 anti-jamming GPS device that meets strict size, weight, power and cost (SWaP-C) requirements and equipping  
 10 all soldiers deployed in the field with these devices are challenging tasks to accomplish.

11 Drone base station (DBS) based communication and soldier position estimation offers inherent solutions to  
 12 the aforementioned problems. First, high altitude DBS deployment reduces the probability of NLoS transmission  
 13 and line-of-sight (LoS) condition dominates the channel between the DBS and the user [6]. Second, GPS of a  
 14 drone is more robust to GPS jamming applied from the ground as the antenna has an unobstructed view of the  
 15 sky, which ensures good signal reception and provides, to some extent, spatial filtering of jamming signals [5].  
 16 Hence, with the help of localization techniques and usage of drones as reference points estimating the locations  
 17 of soldiers becomes possible [7]. In particular, received signal strength (RSS) based localization, which does not  
 18 require hardware modification of drone is an attractive method for this application. Final advantage of the DBS  
 19 use is related to the handling of soldiers' mobility. DBS is able to fly to the new position in order to maximize  
 20 coverage when the soldiers move from one location to another.

21 As there are threats to soldiers in the ground, there are threats to DBSs in the air as well. The authors  
 22 in [3, 8] report that the urban warfare is primarily conducted with small arms such as sniper rifles or machine  
 23 guns. In this respect, we identify that small arm equipped enemy who is trained to shoot down DBS, which  
 24 we call drone shooter thereafter, pose a significant risk in maintaining DBS-based communication service in the  
 25 urban warfare. Therefore, DBS placement decision should be made considering the coverage and drone safety  
 26 requirements with respect to an operation undertaken. This phenomenon complicates the already difficult  
 27 problem of DBSs deployment [9].

28 In this work, we examine the scenario of urban warfare and its challenges from the perspective of wireless  
 29 communication networks. We propose a novel DBS deployment algorithm, which employs both low-cost RSS-  
 30 based technique to estimate soldier positions in the urban environment and utilize k-means clustering supported  
 31 heuristic algorithm which takes into account the presence of drone shooters. We consider air-to-ground Gaussian  
 32 mixture path loss model [6] and derive the maximum likelihood (ML) estimation of the angles between DBSs and  
 33 soldiers, that enables position estimates of soldiers. For the same scenario, we investigate a near-optimal upper  
 34 bound for coverage using a computationally intensive particle swarm optimization (PSO) method. Finally, the  
 35 discussion is provided regarding the deployment decision under two conflicting objectives, namely, minimum  
 36 number of soldiers unserved and maximum probability of DBSs not being hit. To the best of our knowledge,  
 37 this is the first article which investigates the DBSs placement problem considering the requirements of urban  
 38 warfare.

39 Recently, DBS deployment has attracted many researchers. There are diverse use cases for the utilization  
 40 of DBSs and it is considered as an important component in beyond-5G networks [10]. In our previous work, we  
 41 studied fairness-aware multiple DBSs deployment and analyzed the use of the efficient clustering algorithms for  
 42 determining the positions of a number of DBSs in a 3-dimensional (3D) space in order to achieve maximum log-

1 sum data rate. The work in [11] derives the optimal deployment altitude of a single DBS to maximize coverage  
 2 with minimum transmit power. In [12], the backhaul capacity-aware 3D placement of a DBS is considered. The  
 3 authors propose two placement approaches, one maximizes user coverage and the other maximizes the total  
 4 user data rate. [13] studies the placement of a single DBS to maximize network revenue that is defined as the  
 5 number of users covered. The authors in [14] employ PSO technique to find the number of DBSs required and  
 6 their positions to minimize the number of uncovered users. In [15], a polynomial time algorithm aiming to  
 7 minimize number of DBSs needed to cover users is proposed. Here, the problem formulation does not consider  
 8 interference amongst DBSs. The DBSs deployment based on circle packing theory is studied in [16] and [17]. In  
 9 the former work, the positions of DBSs are determined to maximize total coverage with minimum transmission  
 10 power and in the latter, DBSs are placed to maximizes the number of covered users with different quality of  
 11 service requirements. In [18], clustering algorithms are used to position the unmanned aerial vehicle (UAV)  
 12 mounted picocells in a two-tier network. There is also some discussion regarding the effect of user positioning  
 13 error on the received signal strength for users serviced by the UAV picocells. However, the presence of NLoS  
 14 link and interference amongst base stations are ignored. In addition, the assumed user positioning errors are  
 15 not sufficient to investigate network performance in the GPS denied urban environments.

16 RSS-based positioning technique is very attractive for DBS-based soldier positioning application because  
 17 it provides a low cost and easy-to-implement solution. RSS-based positioning does not require antenna arrays  
 18 employed in angle based localization technique [19]. Furthermore, it does not require precise time synchroniza-  
 19 tion that is needed in time-based localization approaches [20]. The use of drones for positioning is studied  
 20 in [21] and [22]. The author in [21] considers a single flying drone equipped with GPS and particle filtering  
 21 algorithm to design RSS-based positioning. In [7], drone based positioning using RSS samples is studied for  
 22 urban environment. The authors derive Cramer-Rao lower bound for the estimated distance as a function of  
 23 the elevation angle and the drone to node distance. However, more realistic Gaussian mixture channel model is  
 24 not considered and formulation of ML estimator is not provided.

25 The rest of the paper is organized as follows. In Section 2, we present the system model. In Section 3, the  
 26 DBSs deployment algorithm which considers the requirements of urban warfare is presented. In Section 4, we  
 27 present numerical simulations and discuss the trade-offs and performance. Finally, in Section 5 we summarize  
 28 our work and discuss the future work.

## 29 **2. System model and assumptions**

30 We focus on a downlink transmission system, where DBSs provide service to the soldiers in urban terrain as  
 31 shown in Figure 1. Using the definitions given in [23], we identify that there are two major zones in urban  
 32 battlefield, theater of operation (TOO) and theater of war (TOW). In our work, friendly force soldiers are  
 33 distributed in the TOO according to the structured group mobility model (SGMM) which is used for modelling  
 34 task oriented node positioning [24, 25]. Drone shooters are distributed uniformly in the TOW. However, to be  
 35 more realistic it is assumed that each soldier has a protected zone around himself, where drone shooters are not  
 36 positioned. The users and drone shooters are assumed to be stationary and the deployment problem is solved  
 37 for this fixed topology.

38 Due to GPS jamming, we consider that soldiers have no access to GPS service, whereas DBSs utilize GPS  
 39 service to locate themselves. We consider both friendly forces and drone shooters are positioned on ground,  
 40 not on rooftops or in buildings. Deploying drone shooters on the rooftops are not feasible as they can be  
 41 easily detected by surveillance drones and become an open target. On the other hand, buildings may limit

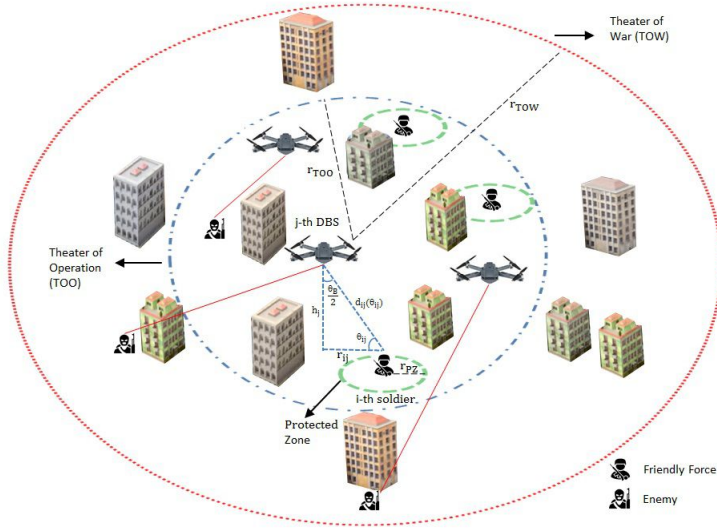


**Figure 1.** System model

1 the shooter's mobility and field of view. DBSs are assumed to be located at a fixed altitude and have same  
 2 transmission power. We also assume that a separate frequency band is allocated for the communication among  
 3 DBSs and enough capacity is provided.

4 DBS deployment consists of two phases. In the first phase, DBSs fly to the fixed points assigned to each  
 5 of them to form an equilateral triangle on the TOO. At the corners of triangle, DBSs collect short pilot signals  
 6 emitted from the radios of soldiers. We assume that all pilot signals reach to DBSs. In the second phase,  
 7 the RSS of pilot signals are used to estimate soldier positions and deployment algorithm determines the final  
 8 positions of DBSs. It is assumed that soldiers are stationary and each soldier is served by a single DBS. We  
 9 consider Time Division Multiple Access (TDMA) for multiple access. In this scheme, each DBS assigns equal  
 10 fraction of time slots to each soldier. We consider that each user is connected to DBS achieving largest Signal  
 11 to Noise Ratio (SNR).

12 The positions of drone shooters are assumed to be obtained via Human Intelligence (HUMINT) network  
 13 [26] or by soldiers who are trained to visually estimate target locations [27] and report to DBSs. Because  
 14 soldiers report the positions relative to their locations, the same error margin is applied to real positions of  
 15 drone shooters. The probability of DBSs not being hit is calculated when they reach their final operational  
 16 positions for providing service to soldiers.

17 We denote soldiers, DBSs and drone shooters by the sets  $\mathcal{U} = \{1, \dots, U\}$ ,  $\mathcal{D} = \{1, \dots, D\}$  and  $\mathcal{T} =$   
 18  $\{1, \dots, T\}$ , respectively. The position of the  $i$ th soldier,  $(x_i^u, y_i^u)$  and  $l$ th drone shooter,  $(x_l^t, y_l^t)$ , are estimated  
 19 and denoted by  $(\hat{x}_i^u, \hat{y}_i^u)$  and  $(\hat{x}_l^t, \hat{y}_l^t)$ , respectively, where  $i \in \mathcal{U}$  and  $l \in \mathcal{T}$ . We denote the 3D position of the  
 20  $j$ th DBS by  $(x_j^d, y_j^d, h_j^d)$  where  $j \in \mathcal{D}$ .

### 21 **2.1. Path loss model**

22 We adopt the Gaussian mixture path loss model proposed in [6], whose simplified version is widely used by  
 23 the researchers for the analysis of DBS placement problems [12–14]. It is important to note that we apply

1 a realistic excess path loss model, which is dependent on the operating frequency, environment and elevation  
 2 angle between the DBS and the soldier. The path loss between the  $i$ th soldier and  $j$ th DBS in the LoS and  
 3 NLoS cases are formulated as,

$$PL_{LoS}^{ij}(\theta_{ij}) = 10\gamma \log \left( \frac{4\pi d_{ij}(\theta_{ij})f_c}{c} \right) + \eta_{LoS}(\theta_{ij}), \quad (1)$$

$$PL_{NLoS}^{ij}(\theta_{ij}) = 10\gamma \log \left( \frac{4\pi d_{ij}(\theta_{ij})f_c}{c} \right) + \eta_{NLoS}(\theta_{ij}), \quad (2)$$

5 where  $\gamma$  is the path loss exponent,  $f_c$  is the operating frequency,  $c$  is the speed of light,  $d_{ij}(\theta_{ij}) = \frac{h_j}{\sin(\theta_{ij})}$   
 6 and  $\theta_{ij} = \arctan \frac{h_j}{r_{ij}}$  are the distance and elevation angle between the soldier  $i$  and DBS  $j$ , respectively where  
 7  $h_j$  is the altitude of the  $j$ th DBS and  $r_{ij}$  equal to  $\sqrt{(x_j^d - x_i^u)^2 + (y_j^d - y_i^u)^2}$  is the horizontal distance between  
 8  $i$ th soldier and the  $j$ th DBS.  $\eta_{LoS}(\theta_{ij})$  and  $\eta_{NLoS}(\theta_{ij})$  are the excess path loss components (in dB) of the LoS  
 9 and NLoS links, respectively.

10 In [6], the excess path loss samples, which are obtained by a ray tracing simulation, are organized in  
 11 terms of the elevation angle. For simplicity, the authors propose to use Gaussian distribution for  $\eta_{LoS}(\theta_{ij})$  and  
 12  $\eta_{NLoS}(\theta_{ij})$  as follows,

$$\eta_{LoS}(\theta_{ij}) \sim \mathcal{N}(\mu_{LoS}, \sigma_{LoS}^2(\theta_{ij})), \quad (3)$$

$$\eta_{NLoS}(\theta_{ij}) \sim \mathcal{N}(\mu_{NLoS}, \sigma_{NLoS}^2(\theta_{ij})), \quad (4)$$

13 where  $\mu_{LoS}$  and  $\mu_{NLoS}$  are the mean excessive losses and  $\sigma_{LoS}$  and  $\sigma_{NLoS}$  are the standard deviations of the  
 14 LoS and NLoS links, respectively. The elevation angle dependent standard deviations of the LoS and NLoS  
 15 links are formulated as,

$$\sigma_{LoS}(\theta_{ij}) = \alpha_1 \exp(-\beta_1 \theta_{ij}), \quad (5)$$

$$\sigma_{NLoS}(\theta_{ij}) = \alpha_2 \exp(-\beta_2 \theta_{ij}), \quad (6)$$

17 where pairs  $(\alpha_1, \beta_1)$  and  $(\alpha_2, \beta_2)$  are frequency and environment dependent parameters for the LoS and NLoS  
 18 links, respectively.

19 The authors in [28] derive a closed form expression for the probability of LoS,

$$p_{LoS}^{ij}(\theta_{ij}) = \frac{1}{1 + a \exp(-b(\theta_{ij} - a))}, \quad (7)$$

20 where  $a$  and  $b$  are environment dependent constants,  $p_{LoS}^{ij}$  is the probability of LoS between  $i$ th soldier and  
 21  $j$ th DBS. The probability of NLoS for the same pair,  $p_{NLoS}^{ij}$ , is calculated as  $1 - p_{LoS}^{ij}(\theta_{ij})$ .

22 Finally, the elevation angle-dependent mean path loss is formulated as:

$$\overline{PL}_{ij}(\theta_{ij}) = PL_{LoS}^{ij}(\theta_{ij})p_{LoS}^{ij}(\theta_{ij}) + PL_{NLoS}^{ij}(\theta_{ij})(1 - p_{LoS}^{ij}(\theta_{ij})). \quad (8)$$

1 **2.2. Modeling soldier distribution**

2 In the urban warfare, small teams are assigned to operations at the tactical level. They operate and move in  
 3 groups to accomplish a given task [29]. The SGMM is used to model node positioning which helps researchers  
 4 to analyze military networks in a more realistic way [24, 25]. In our work, we consider a snapshot of a network  
 5 where a number of soldier groups are distributed in the TOO, which is a cell with radius  $r_{TOO}$ . In this model,  
 6 first group leaders are distributed uniformly in the TOO. Then, soldiers are positioned in reference to their  
 7 group leaders. Figure 2 shows the placement of the  $i$ th soldier with respect to the group leader  $k$ . The  
 8 distance,  $d_i^k$ , and angle,  $a_i^k$ , between the soldier  $i$  and group leader  $k$  are selected from a Gaussian and uniform  
 9 distribution, respectively. In our previous work, we investigated the performance of networks where users are  
 10 uniformly and non-uniformly distributed [9]. In case of non-uniform user distribution, the interference becomes  
 11 more challenging to handle when user groups are in close proximity.

12 **3. DBS deployment in urban warfare**

13 The specific requirements of urban warfare significantly affect the DBSs deployment process. In this regard, we  
 14 first derive the problem of ML estimation of soldier locations based on the RSSs. In addition, we introduce the  
 15 small arm weapon model and derive the probability of DBSs not being hit anticipating the behavior of a drone  
 16 shooter. Then, we present our novel deployment algorithm specifically designed for the challenges of urban  
 17 warfare. In order to understand the coverage performance of our algorithm, we investigate the near-optimal  
 18 deployment of DBSs by proposing 4 different optimization objectives.

19 **3.1. Estimation of soldier locations**

20 Here, we assume that the path loss to each drone is independent. As the drones are significantly apart,  
 21 this is a reasonable assumption. The distribution of path loss is a mixture of two Gaussians (for LoS and  
 22 NLoS) which is presented in [6]. The probability density function of the  $i$ th soldier's path loss vector,  
 23  $\mathbf{PL}_i = [PL_{i1}, PL_{i2}, \dots, PL_{iD}]$ , given the location of the soldier by the elevation angles,  $\theta_i = [\theta_{i1}, \theta_{i2}, \dots, \theta_{iD}]$ ,

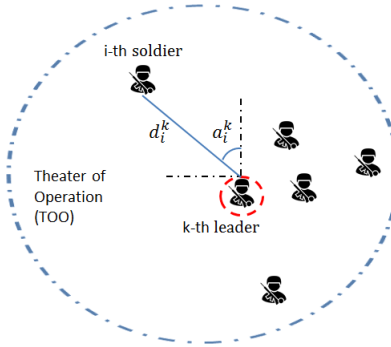


**Figure 2.** Placement of the  $i$ th soldier in reference to the  $k$ th group leader

1 are as follows:

$$f(\mathbf{PL}_i; \theta_i) = \prod_{j=1}^D \left( \frac{p_{LoS}^{ij}(\theta_{ij})}{\sqrt{2\pi\sigma_{LoS}^2(\theta_{ij})}} \exp\left(-\frac{(PL_{ij} - E[PL_{LoS}^{ij}])^2}{2\sigma_{LoS}^2(\theta_{ij})}\right) + \frac{p_{NLoS}^{ij}(\theta_{ij})}{\sqrt{2\pi\sigma_{NLoS}^2(\theta_{ij})}} \exp\left(-\frac{(PL_{ij} - E[PL_{NLoS}^{ij}])^2}{2\sigma_{NLoS}^2(\theta_{ij})}\right) \right) \quad (9)$$

2 where  $E[PL_{LoS}^{ij}]$  and  $E[PL_{NLoS}^{ij}]$  are mean LoS and NLoS path losses respectively.

3 The log-likelihood function is

$$L(\theta_i) = \sum_{j=1}^D \log \left( \frac{p_{LoS}^{ij}(\theta_{ij})}{\sqrt{2\pi\sigma_{LoS}^2(\theta_{ij})}} \exp\left(-\frac{(PL_{ij} - E[PL_{LoS}^{ij}])^2}{2\sigma_{LoS}^2(\theta_{ij})}\right) + \frac{p_{NLoS}^{ij}(\theta_{ij})}{\sqrt{2\pi\sigma_{NLoS}^2(\theta_{ij})}} \exp\left(-\frac{(PL_{ij} - E[PL_{NLoS}^{ij}])^2}{2\sigma_{NLoS}^2(\theta_{ij})}\right) \right) \quad (10)$$

4 Upon maximizing the log-likelihood function, we find the elevation angles of soldier  $i$ .

$$\hat{\theta}_i = \arg \max L(\theta_i). \quad (11)$$

5 Then, the estimated location of soldier  $i$  is found by solving the multilateration problem:

$$(\hat{x}_i^u, \hat{y}_i^u) = \arg \min_{x_i^u, y_i^u} \sum_{j=1}^D \left( \sqrt{(x_j^d - x_i^u)^2 + (y_j^d - y_i^u)^2} - \hat{r}_{ij} \right)^2, \forall i \in U \quad (12)$$

6 where  $\hat{r}_{ij}$  is the estimated distance between the  $i$ th user and  $j$ th DBS and computed using the estimated  
7 elevation angle obtained from Equation 11 as

$$\hat{r}_{ij} = \frac{h_j}{\tan \hat{\theta}_{ij}}. \quad (13)$$

### 8 3.2. Drone shooter model and probability of DBSs not being hit

9 The presence of drone shooters is one of the most challenging issues for sustaining communication service in  
10 urban warfare. Furthermore, as DBSs are shot down, the OPEX (Operational Expenditure) increases and  
11 logistic problems arise. From the communication perspective, shooting down of a single DBS significantly  
12 change the state of network and reconfiguration is needed to compensate for the service loss [30]. Therefore, it  
13 is critical to consider the security of all DBSs while determining their positions. Our proposed algorithm that  
14 we elaborate in the subsequent section takes into account the probability of DBSs not being hit as a security  
15 metric to decide the positions.

16 While calculating the probability of DBSs not being hit, we consider each drone shooter tries to hit the  
17 nearest DBS. The probability of drone shooter seeing the nearest DBS unobstructed is calculated from (7).

18 The probability of DBSs not being hit is calculated as  $p_{noHit} = \prod_{j=1}^D (1 - p_{hit}^j)$ , where  $p_{hit}^j$  is the probability  
19 of  $j$ th DBS being hit that is expressed as  $p_{hit}^j = 1 - \prod_{k \in \mathcal{T}_j} (1 - p_{hit}(d_{jk}) p_{LoS}^{jk})$ , where  $\mathcal{T}_j$  is the set of drone  
20 shooters nearest to DBS  $j$ ,  $p_{hit}(d_{jk})$  is the probability of DBS  $j$  being hit by drone shooter  $k$ , ( $k \in \mathcal{T}$ ),  $d_{jk}$  is  
21 the distance between the DBS  $j$  and drone shooter  $k$ ,  $p_{LoS}^{jk}$  is the probability of LoS between the DBS  $j$  and  
22 drone shooter  $k$ . We assume that drone shooters are equipped with sniper rifles. The work in [31] presents the

1 historical probability of hit values of this weapon at certain distances for stationary man-sized targets. We fit  
 2 the data to the explicit mathematical formula as follows:

$$p_{hit}(d) = \begin{cases} \frac{100 - 5 \exp(0.0028 \times d)}{100}, & \text{if } d < 985m \\ \frac{210.58 \exp(-0.0023 \times d)}{100}, & \text{otherwise.} \end{cases} \quad (14)$$

3 **3.3. DBS deployment based on threat aware user clustering**

4 Here, we describe our proposed DBS deployment algorithm that sequentially executes ML estimator for soldiers'  
 5 locations, k-means clustering and a heuristic which increases  $p_{noHit}$  and at the same time avoid a major  
 6 degradation in the ratio of unserved soldiers,  $N_u$ . Figure 3 shows the general architecture of the proposed  
 7 algorithm, which we call as Threat Aware Clustering with Estimated Positions (TACEP) thereafter. The  
 8 algorithm consists of three phases. In the first phase, for each soldier, RSSs are collected and path losses  
 9 between DBSs and soldier are calculated. Then, ML estimation for finding elevation angles  $\widehat{\theta}_{ij}$ ,  $\forall i \in \mathcal{U}, \forall j \in \mathcal{D}$   
 10 and multilateration for estimating user positions  $\widehat{\mathbf{w}}_i^u = [\widehat{x}_i^u, \widehat{y}_i^u]$ ,  $\forall i \in \mathcal{U}$  are applied respectively. Then the  
 11 estimated soldier positions are clustered to find the positions of DBSs  $\mathbf{w}_j^c = [x_j^c, y_j^c]$ ,  $\forall j \in \mathcal{D}$ . The minimum  
 12 sum-of-squares clustering problem is defined as follows:

$$\begin{aligned} & \min_{\mathbf{w}^c, \mathbf{A}} \sum_{i \in \mathcal{U}} \sum_{j \in \mathcal{D}} A^{ij} \|\widehat{\mathbf{w}}_i^u - \mathbf{w}_j^c\|^2 \\ & \text{subject to} \\ & \sum_{j \in \mathcal{D}} A^{ij} = 1, \quad \forall i \in \mathcal{U} \\ & A^{ij} \in \{0, 1\}, \quad \forall i \in \mathcal{U}, \forall j \in \mathcal{D} \end{aligned} \quad (15)$$

13 where  $\mathbf{w}^c$  is the positions of DBSs,  $A^{ij}$  is a binary variable and equals to 1 if  $i$ th user is associated with  
 14  $j$ th DBS. We adopt Lloyd's algorithm to solve this clustering problem. The algorithm first randomly assigns

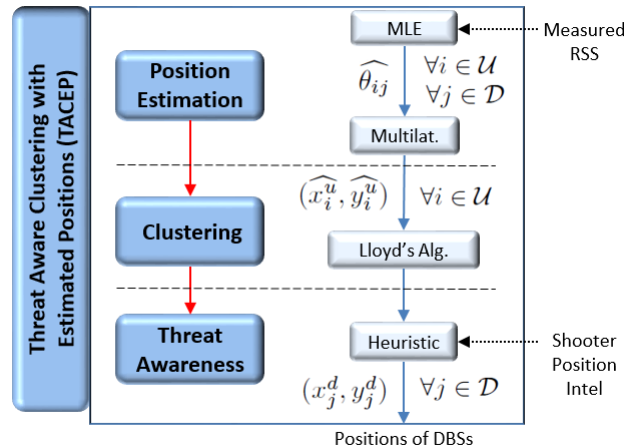


**Figure 3.** Algorithm architecture of TACEP

1 positions to the DBSs. Then, each soldier connects to the nearest DBS and the soldier groups  $\mathcal{S}_1, \dots, \mathcal{S}_D$  are  
 2 formed. The position of each DBS is found by calculating the mean of soldiers' positions connected to the  
 3 DBS. The position update continues until there is no major change in the positions of DBSs. In the final step,  
 4 our proposed iterative threat-aware heuristic approach is applied to find final positions of DBSs  $\mathbf{w}_j^d = [x_j^d, y_j^d]$ ,  
 5  $\forall j \in \mathcal{D}$ . In this approach, first the most vulnerable DBS (the one with the highest hit probability) is found  
 6 and then its new location is calculated by moving DBS by a fixed distance,  $d_h^\Delta$ , away from the closest shooter.  
 7 Next, if new  $p_{noHit}$  is larger than the previous one, the position of DBS is updated. This process continues until  
 8 new  $p_{noHit}$  is not larger than the previous one. The maximum distance between the original (before applying  
 9 heuristic) and new DBS position,  $d_h^{max}$ , is predetermined. If  $d_h^{max}$  is reached for a DBS and it is still the most  
 10 vulnerable one, algorithm considers the second most vulnerable DBS to move.

11 **3.4. Minimum number of unserved soldiers**

12 The challenging nature of urban channel makes the problem of DBS deployment very hard. Randomly changing  
 13 angle-dependent excess losses prevent convergence to an optimal solution for minimizing the number of soldiers  
 14 unserved. However, there are methods which statistically provide better solutions than the others. In our  
 15 investigation, we define 4 different objective functions to achieve a near-optimal solution for minimizing the  
 16 number of unserved soldiers in the GPS-enabled environment. For each case, the positions of DBSs are obtained  
 17 by maximizing the objective function and then the number of unserved soldiers, denoted as  $N_u$ , is determined.  
 18 We adopt PSO algorithm for solving the problems and limit the number of iterations. Our motivation to limit  
 19 the number of iterations is to consider a practical case where the computing resources are restricted as it is in  
 20 the battlefield.

21 We assume soldier-DBS association is performed on the basis of received signal power. Let  $\alpha_i$  be the  
 22 DBS selected by the  $i$ th soldier.

$$\alpha_i = \arg \max_j R_{ij}(x_j^d, y_j^d, h_j^d), \quad (16)$$

23 where  $R_{ij}(x_j^d, y_j^d, h_j^d)$  is the received signal power from the  $j$ th DBS at the  $i$ th soldier terminal and is calculated  
 24 as:

$$R_{ij}(x_j^d, y_j^d, h_j^d) = 10^{\frac{P_T + G_{ij} - \overline{PL}_{ij}}{10}}, \quad (17)$$

25 where  $P_T$  is the transmission power (in dBm) of a DBS,  $G_{ij}$  is the gain of the DBS antenna and is approximated  
 26 by [32].

27 As we indicate in Section 2, the capacity of a DBS is equally shared amongst the soldiers in the time  
 28 domain. Let  $N_s^j$ , be the total number of served soldiers by the  $j$ th DBS.

$$N_s^j = \sum_{i \in U} I_i^j, \quad \forall j \in \mathcal{D}, \quad (18)$$

29 where binary variable  $I_i^j$  defined as:

$$I_i^j = \begin{cases} 1, & \text{if } \alpha_i = j \text{ and } DR_i(\mathbf{x}, \mathbf{y}, \mathbf{h}) > R_{TH} \\ 0, & \text{otherwise.} \end{cases} \quad (19)$$

30 where  $R_{TH}$  is the data rate threshold,  $DR_i(\mathbf{x}, \mathbf{y}, \mathbf{h})$  is the data rate of the soldier  $i$ ,  $(\mathbf{x}, \mathbf{y}, \mathbf{h})$  denotes the

1 positions of all DBSs where  $\mathbf{x} = [x_1^d, \dots, x_D^d]$ ,  $\mathbf{y} = [y_1^d, \dots, y_D^d]$ ,  $\mathbf{h} = [h_1^d, \dots, h_D^d]$ .  $DR_i(\mathbf{x}, \mathbf{y}, \mathbf{h})$  equals to

$$\frac{W}{N_s^{\alpha_i}} \log_2 \left( 1 + \frac{R_{i\alpha_i}(x_{\alpha_i}^d, y_{\alpha_i}^d, h_{\alpha_i}^d)}{N_o W + \sum_{j \neq \alpha_i} R_{ij}(x_j, y_j, h_j)} \right) \quad (20)$$

2 Hence, the number of served soldiers can be found by  $N_s = \sum_{j \in \mathcal{D}} N_s^j$  and the number of unserved soldiers  
3 equals to  $N_u = N - N_s$ . Given the same altitude for DBSs, the following approaches are used to find the  
4 horizontal positions of DBSs with the help of PSO algorithm. We call the algorithms given below as LinKP,  
5 LogKP, CovKP, ClogKP respectively.

6 **3.4.1. Maximizing sum of data rates approach (LinKP)**

$$\begin{aligned} & \arg \max_{\mathbf{x}, \mathbf{y}} \sum_{i \in \mathcal{U}} DR_i(\mathbf{x}, \mathbf{y}, \mathbf{h}) \\ & \text{subject to} \\ & \sqrt{x_j^2 + y_j^2} \leq r_{TOO} \quad \forall j \in \mathcal{D} \end{aligned} \quad (21)$$

7 **3.4.2. Maximizing sum of log data rates approach (LogKP)**

$$\arg \max_{\mathbf{x}, \mathbf{y}} \sum_{i \in \mathcal{U}} \log(DR_i(\mathbf{x}, \mathbf{y}, \mathbf{h})) \quad (22)$$

subject to the same constraint given in Eq. (21)

8 **3.4.3. Maximizing number of served soldiers approach (CovKP)**

$$\arg \max_{\mathbf{x}, \mathbf{y}} \sum_{i \in \mathcal{U}} \sum_{j \in \mathcal{D}} I_i^j \quad (23)$$

subject to the same constraint given in Eq. (21)

9 **3.4.4. Maximizing joint coverage and sum log rate approach (CLogKP)**

10 In each iteration of CLogKP algorithm, the particles with the largest  $N_s$  is found and then the one with the  
11 largest sum log data rate capacity is selected as the global best solution. The constraint given in Eq. (21) is  
12 applied for the positions of DBSs.

13 **4. Simulation results**

14 In this section, we present the performance of our proposed algorithm, named TACEP, and compare its  
15 performance with three different benchmark algorithms. These benchmark algorithms are all threat-unaware.

- 16 • The first benchmark algorithm is soldier location-unaware EQT which simply places the DBSs at the  
17 corners of an equilateral triangle over TOO.
- 18 • Second benchmark is a K-means clustering based algorithm named KCEP. It clusters soldiers based on  
19 the estimated positions and places DBSs at the centers of clusters.

**Table 1.** Simulation Parameters

Parameter	Definition	Value
$U$	Number of Soldiers	80
$D$	Number of DBSs	3
$T$	Number of Drone Shooters	3
$f_c$	Carrier Frequency	2GHz
$r_{TOW}$	Radius of TOW	1500m
$r_{TOO}$	Radius of TOO	1000m
$r_{PZ}$	Radius of PZ	50m
$d_{max}$	Max. dist.	100m
$W$	Bandwidth	20MHz
$N_0$	Noise Power Spectral Density	-170dBm/Hz
$a, b$	Environmental Parameters	9.61, 0.16
$\eta_{LoS}, \eta_{NLoS}$	Mean Path loss	1dB, 20dB
$\theta_B$	DBS Antenna Beamwidth	140°
$P_T$	DBS Transmission Power	30dBm
$R_{TH}$	Data Rate Threshold	500Kbps
$d_h^\Delta, d_h^{max}$	Parameters for Heuristic	20m, 100m
$N_{MC}$	Monte Carlo Simulations	100

1 • The third benchmark algorithm is a version of CLogKP named CLogEP which we explain in this section.  
 2 This serves as a lower bound on the  $N_u$  performance.

3 We use MATLAB as a simulation platform. The simulations are run for 100 different network topologies  
 4 where the soldiers and drone shooters are distributed according to the models given in Section 2. Then, the  
 5 average of  $N_u$  and  $p_{noHit}$  results, which are denoted as  $\overline{N_u}$  and  $\overline{p_{noHit}}$  respectively, are presented. Unless  
 6 stated otherwise the parameters used in the simulations are from Table 1.

7 We will first determine a threat-unaware lower bound for the number of unserved users ( $N_u$ ) performance.  
 8 For this purpose, we will compare the 4 different objective functions for the PSO-based optimization. In Figure  
 9 4,  $\overline{N_u}$  performance of 4 different optimization objectives are shown. Here, the results of the first approach,  
 10 named as LinKP, show that placing DBSs to maximize the sum of data rates is inadequate for achieving the  
 11 minimum  $\overline{N_u}$ . The second approach, LogKP, maximizes the sum of log data rates and provides significantly  
 12 better performance than that of LinKP. As the soldier coverage is the main problem, CovKP is one of the most  
 13 promising methods to find near-optimal results. However, we find that there is a better approach than CovKP.  
 14 As the combination of CovKP and LogKP, CLogKP achieves the best performance among all approaches. In  
 15 this respect, we identify CLogKP and its version named as CLogEP, which uses estimated positions of soldiers  
 16 instead of real positions, as a near-optimal lower bound for the minimum  $\overline{N_u}$ . We provide the results of both  
 17 CLogKP and CLogEP in Table 2, which shows that our proposed RSS-based ML estimator provides a good  
 18 performance for estimating the soldier's positions.

19  $\overline{N_u}$  and  $\overline{p_{noHit}}$  performance of TACEP and comparison algorithms are presented in Figure 5 and Figure  
 20 6, respectively. With respect to  $\overline{N_u}$  performance of the algorithms, the worst results are obtained from EQT  
 21 as expected since it does not consider the locations of soldiers. TACEP and KCEP perform very closely to  
 22 each other. The performance gap between TACEP and CLogEP increases as the DBSs are placed at the higher  
 23 altitudes. The reason is that as the DBSs are deployed at the higher altitudes, the interference becomes more

**Table 2.** Performance results for DBS altitudes 600m and 800m. The close results of CLogEP and CLogKP suggest that our proposed position estimator works efficiently.

Algorithm	$\bar{N}_u$ (600m)	$\bar{\rho}_u$	$\bar{p}_{noHit}$	$\bar{N}_u$ (800m)	$\bar{\rho}_u$	$\bar{p}_{noHit}$
TACEP	1.032	0.013	0.34	3.669	0.045	0.532
KCEP	0.872	0.010	0.279	3.204	0.040	0.485
EQT	3.784	0.047	0.29	8.811	0.110	0.465
CLogEP	0.580	0.007	0.258	1.241	0.015	0.462
CLogKP	0.418	0.005	0.244	1.094	0.013	0.459

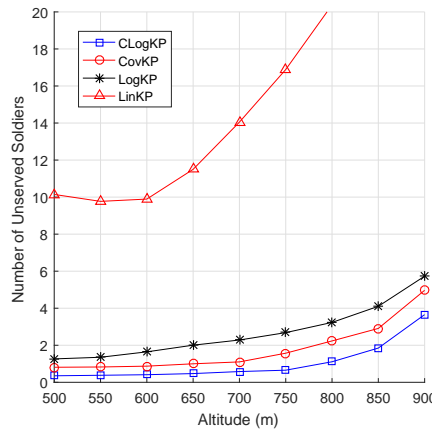


**Figure 4.** Number of unserved soldiers performance for different DBS altitudes. CLogKP achieves the best performance, hence it will be regarded as a lower bound on the  $\bar{N}_u$  performance.

1 difficult to manage and requires more consideration. As presented in Figure 6, TACEP achieves the best  $\bar{p}_{noHit}$   
2 performance which is the primary objective of this algorithm. On the other hand, KCEP performs moderately  
3 well because the centers of soldier clusters are located in the relatively safe regions where shooters are present  
4 with low probability.

5 For the altitudes of 600m and 800m, Table 2 shows the performance of the algorithms in terms of  $\bar{N}_u$ ,  
6  $\bar{p}_{noHit}$  and the average ratio of the number of unserved soldiers, which is denoted as  $\bar{\rho}_u$  and equals to  $\bar{N}_u/N$ .  
7 Considering  $\bar{\rho}_u$  performance at the altitude of 600m, TACEP provides more than three times better performance  
8 than that of EQT and the performance of KCEP and TACEP are very close to each other. The best performance  
9 is provided by CLogEP as expected. On the other hand,  $\bar{p}_{noHit}$  performance of TACEP considerably exceeds  
10 the performance of other algorithms. TACEP outperforms ( $\bar{N}_u$  near-optimal) CLogEP by 31.7% in terms of  
11  $\bar{p}_{noHit}$ . This increase has a significant effect on the mission's outcome considering a DBS serves many soldiers  
12 who need to receive critical ISR information and the available number of DBSs are limited.

13 At the altitude of 800m, KCEP and TACEP again perform very close to each other in terms of  $\bar{\rho}_u$  perfor-  
14 mance. It is observed that CLogEP handles the network better as the altitude increases. This gain is obtained  
15 via CLogEP's interference management capability which comes with increased computational complexity. In  
16 regard to  $\bar{N}_u$  performance, TACEP provides nearly 15% better performance than those of CLogEP and EQT.  
17 This result shows that the efficiency of TACEP is higher at lower altitudes.

18 Trade-off curve of  $\bar{N}_u$  with respect to  $\bar{p}_{noHit}$  performance of the algorithms are shown in Figure 7. It

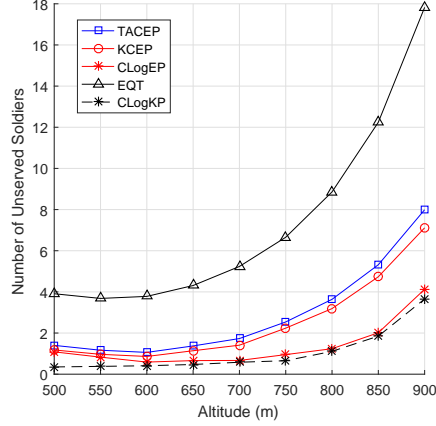


**Figure 5.** Number of unserved soldiers performance versus DBS altitudes. Proposed TACEP has a performance almost equal to KCEP and very close to ClogEP.

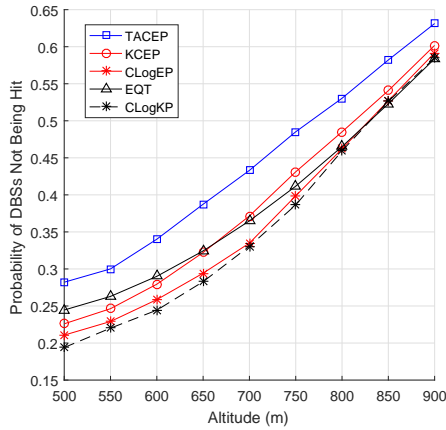


**Figure 6.** Probability of DBSs not being hit performance versus DBS altitudes. Proposed TACEP has a significantly better performance.

1 shows that the best performance is provided by CLogEP, as expected. According to these results, TACEP's  
2 improved  $\bar{p}_{noHit}$  performance does not compromise the near-optimal  $\bar{N}_u$  performance of CLogEP but strikes  
3 a good trade-off between  $\bar{N}_u$  and  $\bar{p}_{noHit}$ . In addition to that, TACEP may be chosen to meet mission specific  
4 requirements such as the DBSs' deployment altitude and security.

5 In the final analysis, we investigate the effect of the number of drone shooters on the probability of DBSs  
6 not being hit. Figure 8 shows that TACEP provides the best performance and outperforms other algorithms  
7 by at least 30% at all altitudes. This shows the efficiency of the TACEP on handling the increasing number of  
8 drone shooters present in the theater of war.

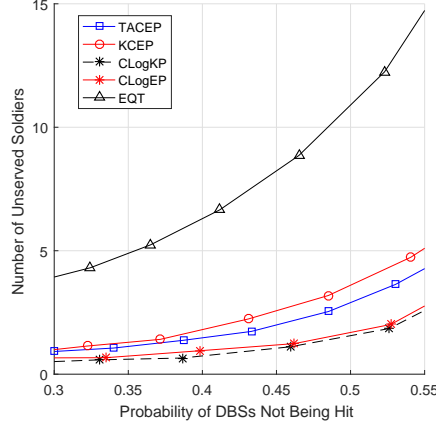


**Figure 7.** The number of unserved soldiers with respect to probability of DBSs not being hit. The results are obtained for the altitude range [500m-900m]. The results show that our proposed fast algorithm strikes a good trade-off.

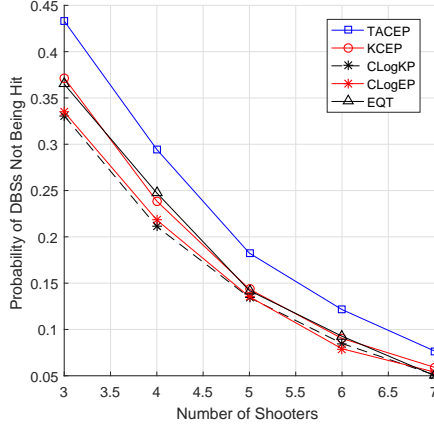


**Figure 8.** Probability of DBSs not being hit performance versus number of drone shooters. DBS altitude is 700m.

## 5. Conclusion

In this work, we have provided a comprehensive examination of the deployment of DBSs in an urban warfare scenario. In this respect, we have introduced specific challenges, namely, a GPS denied environment for the soldiers on the ground and presence of drone shooters aiming to destroy DBSs. Considering these challenges, we have proposed a fast algorithm, referred to as TACEP, to determine the positions of DBSs. Furthermore, we have proposed a PSO based algorithm in order to achieve near-optimal soldier coverage. Simulation results have shown that TACEP outperforms all other algorithms in terms of probability of DBSs not being hit. TACEP also provides a near-optimal coverage performance, when compared with a computation intensive PSO-based algorithm. Future work will consider the case of mobile soldiers and online, adaptive DBS deployment schemes.

1  
References

2 [1] Pendleton G, Bodnar J. Joint urban operations and the NATO urbanisation project. *Three Swords Magazine* 2017;  
3 31: 56–61.

4 [2] NATO. Request for proposal Part 1 bidding instructions. Online Resource 2017.

5 [3] Asymmetric Warfare Group. Modern urban operations lessons learned from urban operations from 1980 to the  
6 present. Technical Report, 2016.

7 [4] Medby JJ, Russell WG. Street Smart: Intelligence preparation of the battlefield for urban operations. Technical  
8 Report MR1287, 2002.

9 [5] Gao GX, Sgammini M, Lu N, Kubo N. Protecting GNSS Receivers From Jamming and Interference. *Proceedings*  
10 of the IEEE 2016; 104: 1327–1338.

11 [6] Al-Hourani A, Kandeepan S, Jamalipour A. Modeling air-to-ground path loss for low altitude platforms in urban  
12 environments. In: *IEEE Global Communications Conference (GLOBECOM)*; 8–12 December 2014; Austin, TX,  
13 USA: IEEE. pp. 2898–2904.

14 [7] Sallouha H, Azari MM, Chiumento A, Pollin S. Aerial anchors positioning for reliable RSS-based outdoor localization  
15 in urban environments. *IEEE Wireless Communications Letters* 2018; 7: 376–379.

16 [8] Edwards SJA. Mars Unmasked: The changing face of urban operations. Technical Report MR1173, 2000.

17 [9] Akarsu A, Girici T. Fairness aware multiple drone base station deployment. *IET Communications* 2018; 12: 425–431.

18 [10] Mozaffari M, Saad W, Walid B, Nam YH, Debbah M. A tutorial on UAVs for wireless networks: applications,  
19 challenges, and open problems. *IEEE Communications Surveys & Tutorials* 2019; Early access.

20 [11] Mozaffari M, Saad W, Bennis M. Drone small cells in the clouds: Design, deployment and performance analysis.  
21 In: *IEEE Global Communications Conference (GLOBECOM)*; 6–10 December 2015; San Diego, CA, USA: IEEE.  
22 pp. 1–6.

23 [12] Kalantari E, Shakir MZ, Yanıkömeroğlu H, Yongaçoglu A. Backhaul-aware robust 3D drone placement in 5G+  
24 wireless networks. In: *IEEE International Conference on Communications Workshops (ICC Workshops)*; 21–25 May  
25 2017; Paris, France: IEEE. pp. 109–114.

26 [13] Bor-Yaliniz RI, El-Keyi A, Yanikomeroglu H. Efficient 3-D placement of an aerial base station in next generation  
27 cellular networks. In: *IEEE International Conference on Communications (ICC)*; 22–27 May 2016; Kuala Lumpur,  
28 Malaysia: IEEE. pp. 1–5.

29 [14] Kalantari E, Yanıkömeroğlu H, Yongaçoglu A. On the number and 3D placement of drone base stations in wireless  
30 cellular networks. In: *IEEE 84th Vehicular Technology Conference (VTC-Fall)*; 18–21 September 2016; Montreal,  
31 QC, Canada: IEEE. pp. 1–6.

32 [15] Lyu J, Zeng Z, Zhang R, Lim TJ. Placement optimization of UAV-mounted mobile base stations. *IEEE Wireless  
33 Communications Letters* 2017; 21: 604–607.

34 [16] Mozaffari M, Saad W, Bennis M, Debbah M. Efficient deployment of multiple unmanned aerial vehicles for optimal  
35 wireless coverage 2016. *IEEE Communications Letters*; 20: 1647–1650.

36 [17] Alzenad M, El-Keyi A, Yanıkömeroğlu H. 3D placement of an unmanned aerial vehicle base station for maximum  
37 coverage of users with different QoS requirements. *IEEE Wireless Communications Letters* 2018; 7: 38–41.

38 [18] Galkin B, Kibilda J, DaSilva LA. Deployment of UAV-mounted access points according to spatial user locations in  
39 two-tier cellular networks. In: *IEEE Wireless Days*; 23–25 March 2016; Toulouse, France: IEEE. pp. 1–6.

40 [19] Yang C, Shao HR. WiFi-based indoor positioning. *IEEE Communications Magazine* 2015; 53: 150–157.

41 [20] Wang Y, Ma X, Leus G. Robust time-based localization for asynchronous networks. *IEEE Transactions on Signal  
42 Processing* 2011; 59: 4397–4410.

1 [21] Caballero F, Merino L, Maza I, Ollero A. A particle filtering method for wireless sensor network localization with an  
2 aerial robot beacon. In: IEEE International Conference on Robotics and Automation; 19-23 May 2008; Pasadena,  
3 CA, USA: IEEE. pp. 596–601.

4 [22] Ouyang RW, Wong AKS, Lea CT. Received signal strength-based wireless localization via semidefinite programming:  
5 noncooperative and cooperative schemes. IEEE Transactions on Vehicular Technology 2010; 59: 1307–1318.

6 [23] US Army forces. Decisive force: the army in theater operations. Technical Report FM 100-7, 1995.

7 [24] Blakely K, Lowekamp B. A structured group mobility model for the simulation of mobile ad hoc networks. In:  
8 Proceedings of the Second International Workshop on Mobility Management and Wireless Access Protocols; 1–1  
9 October 2004; Philadelphia, PA, USA: ACM. pp. 111–118.

10 [25] Zheng H, Shi J, Cao L. Group-mobility-aware spectrum management for future digital battlefields. In: IEEE Military  
11 Communications Conference (MILCOM); 23–25 October 2006; Washington, DC, USA: IEEE. pp. 1–7.

12 [26] Howcroft J. Intelligence challenges in urban operations. Online Resource 2014.

13 [27] Thompson TJ. Range estimation training and practice: A state of the art review. Technical Report, 1982.

14 [28] Al-Hourani A, Sithamparanathan K, Lardner S. Optimal LAP altitude for maximum coverage. IEEE Wireless  
15 Communications Letters 2014; 3: 569–572.

16 [29] Vautravers A. Military Operations in Urban Areas. International Review of the Red Cross 2010; 878: 437–452.

17 [30] Akarsu A, Girici T. Failure aware deployment of drone base stations. In: Telecommunications Forum (TELFOR);  
18 20–21 November 2018; Belgrade, Serbia: IEEE. pp. 1–4.

19 [31] Isby DC. Weapons and Tactics of the Soviet Army. Technical Report, 1981.

20 [32] Balanis CA. Antenna Theory: Analysis & Design. John Wiley & Sons, 1997.